

# Investigating and Modeling the Regulation of Extracellular Antibiotic Resistance Gene Bioavailability by Naturally Occurring Nanoparticles

Nadratun N. Chowdhury,\* Ethan Hicks, and Mark R. Wiesner



Cite This: *Environ. Sci. Technol.* 2022, 56, 15044–15053



Read Online

ACCESS |

Metrics & More

Article Recommendations

Supporting Information

**ABSTRACT:** Extracellular antibiotic resistance genes (eARGs) are widespread in the environment and can genetically transform bacteria. This work examined the role of environmentally relevant nanoparticles (NPs) in regulating eARG bioavailability. eARGs extracted from antibiotic-resistant *B. subtilis* were incubated with nonresistant recipient *B. subtilis* cells. In the mixture, particle type (either humic acid coated nanoparticles (HASNPs) or their micron-sized counterpart (HASPs)), DNase I concentration, and eARG type were systematically varied. Transformants were counted on selective media. Particles decreased bacterial growth and eARG bioavailability in systems without nuclease. When DNase I was present ( $\geq 5 \mu\text{g/mL}$ ), particles increased transformation via chromosomal (but not plasmid-borne) eARGs.

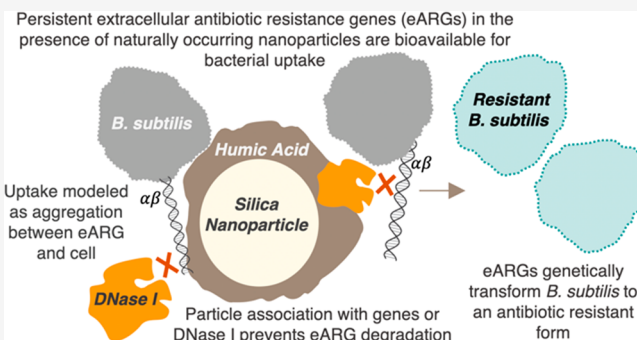
HASNPs increased transformation more than HASPs, indicating that the smaller nanoparticle with greater surface area per volume is more effective in increasing eARG bioavailability. These results were also modeled via particle aggregation theory, which represented eARG–bacteria interactions as transport leading to collision, followed by attachment. Using attachment efficiency as a fitting factor, the model predicted transformant concentrations within 35% of experimental data. These results confirm the ability of NPs to increase eARG bioavailability and suggest that particle aggregation theory may be a simplified and suitable framework to broadly predict eARG uptake.

**KEYWORDS:** antimicrobial resistance, extracellular DNA, nanoparticles, particle aggregation, horizontal gene transfer

## 1. INTRODUCTION

The global rise in antibiotic resistance has led to worldwide increases in mortality, morbidity, and economic costs.<sup>1–6</sup> Mobile genetic elements, which are segments of DNA that can transfer genetic information between bacterial cells, may carry resistance genes and contribute to the proliferation of resistance in microbial populations. These mobile genetic elements include extracellular antibiotic resistance genes (eARGs), which can transfer resistance traits between cells. eARGs have been quantified in freshwater,<sup>7–9</sup> sediment,<sup>10,11</sup> animal feed operations,<sup>6,12</sup> drinking water treatment plants,<sup>6,13</sup> and wastewater treatment plants,<sup>14–17</sup> among other environments. eARGs are part of a larger subset of extracellular DNA (eDNA) which is naturally abundant and has been detected in soil environments at concentrations up to  $200 \mu\text{g/g}$ .<sup>18</sup> The environment contains naturally competent bacterial species that may take up eARGs and incorporate them into their genomes via a horizontal gene transfer process called natural transformation.<sup>19</sup>

Natural transformation is a significant ecological phenomenon which contributes to an extensive microbial gene network. This environmental process has been detected in



situ<sup>19,20</sup> and characterized on the bench-scale.<sup>18,21</sup> The significance of this process is notably enhanced by the interaction of extracellular genes with environmental components. Indigenous nucleases, whose concentrations correlate with microbial abundance in the environment, are capable of degrading significant concentrations of eDNA.<sup>22,23</sup> Environmental components can play a role in protecting eARGs from degradation by such environmentally ubiquitous nucleases and potentially increase the likelihood of the interaction between bacteria and full genes. In nuclease-containing systems, eDNA bound to natural substances such as montmorillonite,<sup>24</sup> illite,<sup>25</sup> humic acid,<sup>26</sup> and sand<sup>27</sup> have demonstrated the capacity to transform bacteria at greater rates than free eDNA. Thereby, it

**Special Issue:** Antimicrobial Resistance in the Environment: Informing Policy and Practice to Prevent the Spread

**Received:** April 22, 2022

**Revised:** June 20, 2022

**Accepted:** July 7, 2022

**Published:** July 19, 2022



is reasonable to consider particle-association as a factor in determining the rate of natural transformation.

Among the particles that may associate with eDNA are naturally ubiquitous nanoparticles (NPs) which have been shown to irreversibly bind eARGs<sup>28</sup> and protect them from enzymatic degradation.<sup>29</sup> Based on these findings, this work hypothesizes that NPs may also mediate natural transformation. The ability of NPs, compared to larger particles, is important to study because nanoemergent traits, such as increased surface area to volume ratios, may facilitate interaction with biological components. NPs also tend to be more mobile<sup>30</sup> and bioavailable<sup>31</sup> than their larger counterparts and may impact eARGs behavior in yet unknown ways.

To characterize the role of NPs in regulating eARG bioavailability, this work reports on (1) the measurement of natural transformation rates of bacteria via eARGs sorbed to particles of various sizes (nano- and micron-scale) and (2) models formulated to describe transformation rates under a broad range of conditions. Culture-based methods were used to quantify transformation of naturally competent *B. subtilis* by various eARGs extracted from *B. subtilis* and pre-equilibrated with nucleases and humic acid coated silica particles. It was hypothesized that the nanoscale silica particle would be most effective at facilitating transformation because it has greater total surface for gene or bacteria attachment. A simplified experimental system that eliminates much of the biological complexity of realistic environments (i.e., diversity of microbiomes, presence of reactive oxygen species (ROS), variation in nuclease concentration, etc.) was used to systematically evaluate the interactions between eARGs, NP, and bacteria.

The experimental transformation rates obtained were also used to construct a model describing natural transformation as an aggregation process between eARGs (free and sorbed) and bacteria. Particle aggregation theory, initially theorized by Smulochowski,<sup>32</sup> has been used to inform models of various environmental processes (i.e., phage-host attachment<sup>33,34</sup>). It was hypothesized here that particle-particle interactions described by Smulochowski's theory may realistically depict the attachment of eDNA to bacterial surfaces. Like the experimental system, the model developed here assumes a simplified system without considering various complexities of real environmental systems. Therefore, it can evaluate the importance of fundamental particle-eDNA-bacteria interactions on rates of genetic uptake without the need for extensive experimental data. This work develops an initial understanding of eARG behavior with regard to bacteria and NPs and is a baseline from which to evaluate how eARGs may propagate antibiotic resistance in the environment.

## 2. METHODS

**2.1. Bacterial Strains.** All bacteria used in experimentation were *Bacillus subtilis* 168 from the *Bacillus* Genetic Stock Center (BGSC) (Ohio State University). Because horizontal gene transfer via transformation is more likely to occur between genes of the same species,<sup>23</sup> both eARGs and recipient cells were from the species *B. subtilis* to ensure sufficient transformation rates. Strains used include *B. subtilis* 1A1 (nonresistant), *B. subtilis* 1A189 (multidrug, including acriflavine, resistant), *B. subtilis* 1A354 (sulfanilamide resistant), and *B. subtilis* 1A491 (trimethoprim resistant).

*B. subtilis* 1A189 includes a point mutation (*acfa*, which is an Adenine-Thymine base-pair deletion) in its genomic DNA within the promoter region of the 1203 bp *blt* gene. The *blt*

gene is part of the *bltR-blt-bltD* genome segment. The full sequence, location of each gene, and location of the mutation are given in the Supporting Information (Text S1), with the mutant genome segment codes for efflux-mediated resistance to multiple antibiotics including acriflavine.<sup>1</sup>

*B. subtilis* 1A354 may include multiple plasmid-bound sulfanilamide resistance genes, such as *sul1*, *sul2*, or *sul3*. These *sul* genes code to produce an alternative dihydropteroate synthetase with low sulfanilamide affinity.<sup>35,36</sup> *B. subtilis* 1A491 includes multiple mutations, likely substitutions within the *dfrA24* gene,<sup>37,38</sup> and is trimethoprim resistant by way of modifying the dihydrofolate reductase.<sup>38</sup> These strains were chosen so that their mutations could be compared. All strains were revived and cultured on nutrient agar at 37 °C according to BGSC instructions. The strains used and their properties are summarized in the Supporting Information (Table S1).

**2.2. DNA Extraction and PCR Amplification.** Genomic DNA from each antibiotic resistant *B. subtilis* strain was extracted using the DNeasy UltraClean Microbial Kit from Qiagen (Hilden, Germany), according to the manufacturer's instructions. Extraction was confirmed by quantification of DNA using the Qubit 2.0 fluorometer from Life Technologies (Carlsbad, CA). Fragments of the gene *blt* were amplified from extracted *B. subtilis* 1A189 DNA using the polymerase chain reaction (PCR). The PCR protocol is given in the Supporting Information (Text S2). Five fragments of various sizes (191 bp, 400 bp, 906 bp, 1100 bp, and 1500 bp) were extracted. Each fragment was chosen, using widely available *B. subtilis* 168 sequencing data, such that the point mutation *acfa* is symmetrically flanked. The locations and sizes of fragments, along with primers, are demonstrated in the Supporting Information (Text S1, Figure S1). These fragments were prepared to test for the impact of flanking region length on transformation. The 906 bp fragment was also amplified as single stranded DNA (ssDNA) to test the impact of strand conformation.

**2.3. Particle Preparation.** Two model colloids were used in transformation studies: 100 nm silica nanoparticles (Nanocomposix, San Diego, CA) surface functionalized with humic acid (Sigma, St. Louis, MO) (HASNPs) and 1 μm silica nanoparticles (Nanocomposix, San Diego, CA) surface functionalized with humic acid (HASPs). The silica particles used were spherical and made up of an amorphous network of silicon and oxygen. HASNPs were used as model NPs because sorption of eDNA to bare silica was previously reported to be minimal and the functionalization with humic acid allowed for significant eDNA sorption.<sup>28</sup> HASPs were used as the micron-sized equivalent for comparison.

HASNPs and HASPs were prepared as described in the Supporting Information (Text S3). They were characterized for their hydrodynamic diameter and calculated zeta potentials by dynamic light scattering (DLS). These results are given in the Supporting Information (Text S4, Table S2, and Figure S2).

**2.4. DNA Sorption and DNase I Exposure.** eARGs were equilibrated with particles and DNase I prior to natural transformation assays. DNase I was added so that the impact of particle-mediated protection of genes<sup>29</sup> could be assessed on transformation. The DNA sorption and DNase I exposure procedure is described in the Supporting Information (Text S5). Extracted *B. subtilis* 1A189 DNA was exposed to a range of DNase I concentrations (0, 0.5, 1, 5, 10, and 20 μg/mL). Previously, it was reported that the amount of persistent eDNA

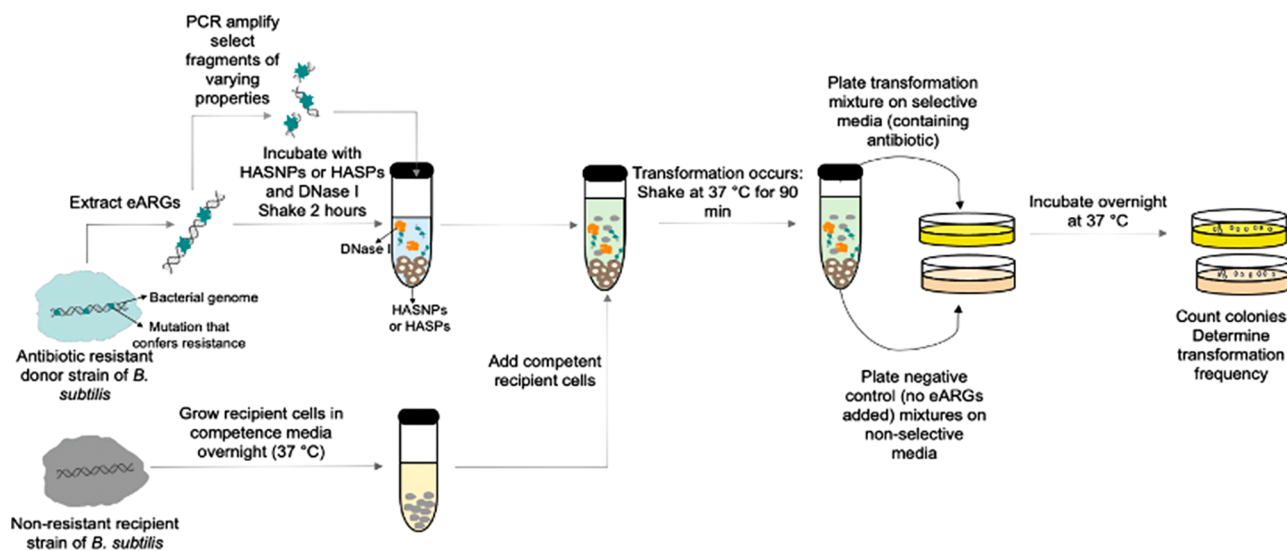


**Figure 1.** Schematic of natural transformation assay in which eARGs extracted from donor bacteria are amplified by PCR and used to transform nonresistant recipient bacterial cells.

varied significantly across this range of DNase I exposures.<sup>29</sup> Therefore, this full range was tested here to evaluate how changes in persistence may correlate with changes in bioavailability.

The remaining eARGs (the 5 PCR amplified *blt* fragments, the single stranded 906 bp *blt* fragment, and DNA extracted from *B. subtilis* 1A354 and *B. subtilis* 1A491) were then prepared (exposed to a single DNase I concentration (1  $\mu$ g/mL)) to determine impacts of eDNA properties on transformation. At this DNase I concentration, most free eDNA is fully degraded,<sup>25,39,40</sup> and remaining eDNA are likely particle-associated. Using this DNase I concentration ensures a comparison between the impact of gene properties on particle-free and particle-mediated transformation.

For each eARG type, the adsorption and exposure processes were performed for each particle condition (HASNP, HASP or particle-free) in triplicate. Concentrations of DNA used were 2  $\mu$ g/mL, and concentrations of particles used were 0.25 g in 500  $\mu$ L of solution. This particle concentration was used because it provides sufficient surface area for the dosed eDNA to sorb.<sup>28</sup> It was used to clearly discern impacts of nanoparticles on eARG behavior and to represent a system where naturally occurring nano-SiO<sub>2</sub> with organic matter is abundant.

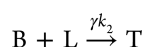
**2.5. Natural Transformation Assay.** Transformation tests were performed with nonantibiotic resistant *B. subtilis* 1A1 as the recipient cell. Transforming eDNA was extracted from *B. subtilis* 1A189 for tests with DNase I variations, PCR amplified fragments of *B. subtilis* 1A189 for tests with variations in fragment size and strand conformation, *B. subtilis* 1A354 for testing sulfanilamide resistance, and *B. subtilis* 1A491 for testing trimethoprim resistance. The full transformation assay was adapted from He et al. (2019)<sup>1</sup> and is described in the Supporting Information (Text S6, Figure S3). A schematic summarizing the full transformation procedure is given in Figure 1.

**2.6. Model Simulations.** **2.6.1. Model Formulation.** Natural transformation of particle associated eARGs is modeled through three reactions.

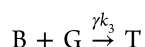
Reaction 1



Reaction 2



Reaction 3



N, G, L, B, and T represent the mass concentration of nanoparticles, free eARGs, sorbed eARGs, untransformed bacterial cells, and transformed bacterial cells, respectively. **Reaction 1** describes a reversible adsorption at equilibrium between eARGs and particles. **Reaction 2** and **Reaction 3** represent the uptake of free and dissolved genes, respectively, by bacteria as a nonreversible “aggregation” between DNA and cells.

The rate constants  $k_2$  and  $k_3$  are mass-based second-order reaction rate constants which describe the loss of free bacteria and the formation of transformed bacteria through the attachments of the genes and the gene–particle ligands to bacteria. However, to present the model on a population basis, which is necessary for Smoluchowski-type modeling, the mass-based reaction rates  $k_2$  and  $k_3$  must be transformed into Smoluchowski-type population-based reaction (aggregation) rates which mirror the gene–bacteria and gene–ligand–bacteria attachment.

There are two parameters that encompass a modified Smoluchowski approach to tracking particle aggregation:  $\alpha$  (attachment efficiency) and  $\beta$  (collision frequency).  $\beta$  (with units of inverse particle concentration per time) represents the frequency of particle collisions via three pathways: Brownian motion (BR), differential settling (DS), and shearing (S). Here, the rectilinear model<sup>32</sup> is utilized to calculate  $\beta$ . The effect of compressing streamlines during particle approach is therefore not considered. For spherical particles, this hydrodynamic retardation has the effect of significantly overestimating collisions between particles of very different sizes. However, given the nonspherical nature of the particles involved and the assumptions applied, the use of the curvilinear model for the collision kernel was not considered warranted. The collision frequencies from the transport pathways are additive. The full analytical equations for  $\beta$  are

provided in the Supporting Information (Text S7.1, Equation S1).

Attachment upon collision between eARGs and bacteria is a function of several factors, such as the binding sites available on the cell surface,<sup>41</sup> the presence of protein-like binding factors,<sup>42</sup> pH,<sup>43</sup> and sequence homology.<sup>19,44</sup> The probability that a particle or gene will attach to a bacterium is depicted in this model by  $\alpha$ . The theory for calculating  $\alpha$  is highly restrictive; therefore, it is treated as a fitting factor that corrects for the assumption of rectilinear particle trajectories. Furthermore, whether or not an attached gene is integrated into the chromosome is dependent on various factors, such as divalent cation concentration,<sup>45</sup> the presence of competence proteins,<sup>46</sup> and sequence homology.<sup>43</sup> Therefore, the additional correction factor  $\gamma$  is used to convert  $\alpha\beta$  to the number of attachments that subsequently lead to transformed bacteria.

With these factors in mind, along with assumptions of no cell growth or decay, the following population balances (based on Reaction 1–Reaction 3) and expressions for  $k_2$  and  $k_3$  can be made:

$$\frac{dB}{dt} = -\gamma(k_2 LB + k_3 GB) \quad (1)$$

$$\frac{dT}{dt} = \gamma(k_2 LB + k_3 GB) \quad (2)$$

$$k_2 = \frac{\alpha_{LB}\beta_{LB}}{\gamma\rho_L V_L} [ = ] \frac{L^3}{M \times T} \quad (3)$$

$$k_3 = \frac{\alpha_{GB}\beta_{GB}}{\gamma\rho_G V_G} [ = ] \frac{L^3}{M \times T} \quad (4)$$

where  $k_2$  describes the aggregation between attached genes and bacteria and  $k_3$  describes the aggregation between dissolved genes and bacteria.

Reaction 1 is assumed to occur rapidly, such that the fraction of sorbed eARGs,  $f_p$ , can be estimated using partition coefficients,  $P$ , calculated as the slope of the linear portion of the pertinent sorption isotherms.

$$f_p = \frac{PN}{1 + N} \quad (5)$$

The model also seeks to represent the loss of genetic material due to enzymatic degradation. This is assumed to occur as a pseudo-first order reaction with degradation rate constants  $k_{d,1}$  and  $k_{d,2}$ , which describe degradation kinetics of sorbed and free eARGs, respectively. These rate constants can be determined from kinetic eARG degradation data.

A mass balance can account for the total amount of genetic material, or  $c_T$ .

$$\frac{dc_T}{dt} = -k_{d,1}f_p c_T - k_{d,2}(1 - f_p)c_T \quad (6)$$

**2.6.2. Calibration.** Model parameters were estimated from literature and experimental data. The values and methods used to estimate them are summarized in the Supporting Information (Text S7.2). These values were used to convert transformant counts in CFU/mL to mass concentration. Calibration consisted of determining values for  $\alpha$  that yielded a satisfactory fit to experimental data using *B. subtilis* 1A189 genomic DNA to transform *B. subtilis* 1A1, in a system with 1  $\mu$ g/mL DNase I over 90 min. Calibrations were performed for

both HASNP and particle-free data sets (Figure 2).  $\alpha_{GB}$  was calibrated to match the experimental  $T$  determined in particle-

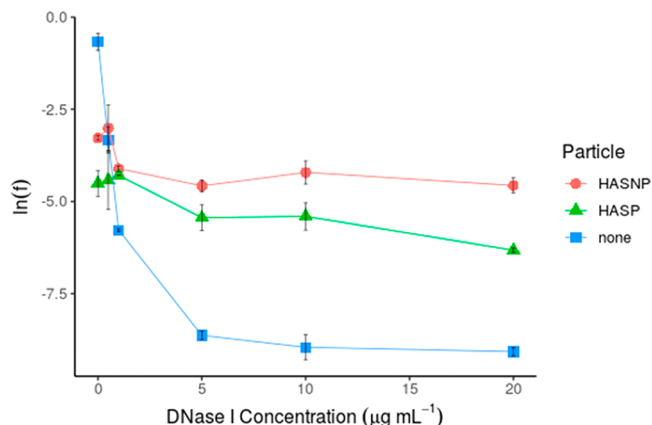


**Figure 2.** Transformation frequencies ( $f$ ) in systems with varying DNase I concentrations and either HASNPs, HASPs, or no particles.

free systems. Then, with  $\alpha_{GB}$  held constant, the initial particle concentration  $N_0$  was set to a value of 0.5 g/mL, and  $\alpha_{LB}$  was iterated until  $T$  matched experimental values at 90 min.

**2.6.3. Validation.** The model was validated using transformation assays in HASP systems (using *B. subtilis* 1A189 genomic DNA to transform *B. subtilis* 1A1 in a system with 1  $\mu$ g/mL DNase I over 90 min (Figure 2). All parameters were held constant except  $d_L$ , which was changed to 2.246  $\mu$ m for HASPs as determined by Zetasizer (Malvern Panalytical, Malvern, U.K.) measurements. Since it is reasonable to assume that less eARGs adsorb to the larger particle, which has a smaller specific surface area, the partition coefficient determined for the NPs was adjusted for the micron-scale HASPs by scaling the specific surface area (see the Supporting Information (Text S7.3). The model-predicted  $T$  and the experimental  $T$  after 90 min were compared.

**2.7. Analysis.** All data points were collected in triplicate, and the standard error of the mean was determined. The significance of particle addition, resistance gene type, and/or DNA properties on transformation rates was determined by analysis of variance (ANOVA). Significance was assumed at  $p < 0.05$ .

Model parameters (summarized in the Supporting Information (Table S3) were used to determine collision frequency parameters and rate constants. The mass and population balances in eqs 1, 2, and 6 were solved numerically using Euler integration using MAT-LAB R2019a. The MAT-LAB code is given in the Supporting Information (Text S8).

### 3. RESULTS AND DISCUSSION

**3.1. Transformation Assays.** **3.1.1. Particle Effects on Bacterial Concentration.** With the addition of either HASNPs ( $p < 0.04$ ) or HASPs ( $p < 0.05$ ), the total concentration of bacteria decreased significantly (Figure S4). This implies that particles inhibited the growth of bacteria. In some cases, decreased bacterial growth has been observed in bacteria associated with particle surfaces due to less cell surface available for substrate uptake,<sup>47,48</sup> higher maintenance coefficient,<sup>47</sup> or substrate transport limitations.<sup>49</sup> Such phenomena may be contributing to decreased *B. subtilis* growth in association with HASPs and HASNPs.

**3.1.2. Particle Effects on Transformation in Systems with DNase I.** With no DNase I present, transformation frequencies ( $f$ ) are highest for particle-free systems (Figure 2). A significant decrease in  $f$  is observed with the addition of HASPs ( $p < 0.0008$ ) or HASNPs ( $p < 0.0004$ ). This implies that particles may hinder transformation in systems without nuclease. Because the concentration of eDNA used in this study was significantly lower than the maximum adsorption capacities previously reported for eDNA to HASNPs and because most eDNA is reported to bind irreversibly to HASNPs,<sup>28</sup> it is reasonable to assume that eARGs in particle systems were bound to the particles. Previous studies have suggested that a portion of particle-bound DNA can be removed and taken up by bacterial cells, while some portion of particle-bound DNA cannot be.<sup>23,25,50,51</sup> Sorption of eDNA to the particle surface may decrease the total fraction of bioavailable genes. This observed inhibitory effect on transformation is greater for HASPs than HASNPs ( $p < 0.03$ ). In some cases, bacterial uptake is more efficient when bacteria is bound directly to the mineral surface.<sup>52</sup> If NPs have greater surface area per volume, they may also have more bacterial binding sites. Because NPs are smaller, they also may be less sterically hindered than larger particles from binding on a small bacterium.

At 0.5  $\mu\text{g}/\text{mL}$  DNase I concentrations, the inhibitory effect of particles is no longer observed ( $p < 0.3$ ). When DNase I concentrations are increased to 1  $\mu\text{g}/\text{mL}$  or more, there are significant increases in  $f$  observed for both HASP ( $p < 3 \times 10^{-6}$ ) and HASNP ( $p < 3 \times 10^{-5}$ ) systems, as compared to particle-free systems. This implies particles may increase natural transformation frequencies when sufficient nuclease is present. The mechanism of this particle effect is not yet clear. The advantage conferred by particles in the presence of DNase I may be due to particles associating with nucleases and deactivating them, allowing more free eDNA to persist and be taken up by bacteria. It is also possible that particles protect eDNA from degradation and then are desorbed before they are taken up by microbes. Significant desorption of eDNA from HASNP surfaces has been previously observed.<sup>28</sup> It has been documented in previous work that indigenous nuclease can degrade eDNA dosed into environmental samples at similar concentrations as tested here. Therefore, it is possible that high enough DNase I concentrations could be present in certain natural environments to create an advantage for particle-bound eARGs. Further study is required to determine this.

Additionally, transformation frequency was significantly greater in HASNP systems compared to HASP systems at up to 20  $\mu\text{g}/\text{mL}$  DNase I concentrations ( $p < 0.001$ ). This may be due to a difference in sorption capacities of the particles. Previous work has demonstrated high sorption capacity of eDNA to HASNPs (~50  $\mu\text{g}/\text{g}$ )<sup>28</sup> and to DNase I (~54  $\mu\text{g}/\text{g}$ ).<sup>39</sup> The high sorption capacity of NPs may be due to the fact they, compared to larger particles, have a greater surface area per volume and potentially a greater number of binding sites that may allow eARGs or nucleases to bind.

Moreover, the production of reactive oxygen species (ROS) may play a role in upregulating competence genes and facilitating gene transfer.<sup>53–57</sup> While there has been no evidence that  $\text{SiO}_2$  produces ROS in associated bacteria, humic acids are known photocatalytic producers of singlet oxygen and may have played a role in facilitating gene uptake.<sup>58</sup> This effect may have been more pronounced for

HASNPs, which have a greater surface area to volume ratio and can bind comparatively more organics than HASPs.

**3.1.3. Effect of eARG Fragment Size and Strand Conformation.** No significant effect of fragment size (in eARG fragments with a symmetrically flanked point mutation) was observed in the size range tested, in systems with HASNPs ( $p < 0.2$ ), HASPs ( $p < 0.8$ ), or no particles ( $p < 0.8$ ) (Figure 3A). Larger flanking regions have been shown to aid transformation by facilitating homologous recombination.<sup>59</sup> Studies that have demonstrated such correlations have used donor fragments that range up to hundreds of thousands of base pairs long.<sup>60</sup> Perhaps, the variation in the flanking region size tested here was not large enough to show significant differences in transformation frequency. Also, none of the PCR-amplified fragments tested included the full *blt* gene. Differences in transformation may have been more easily discernible with the full gene, as bacterial populations are more likely to retain a gene if taken up in entirety.<sup>61–63</sup>

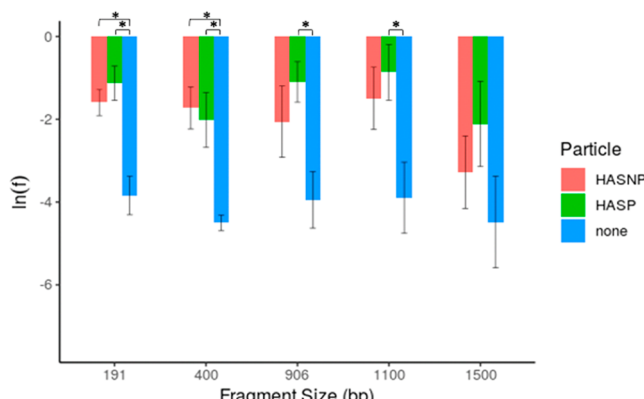
No significant differences in transformation frequencies via double-stranded DNA (dsDNA) and single-stranded DNA (ssDNA) were observed for systems with HASNPs ( $p < 0.7$ ), HASPs ( $p < 0.1$ ), or no particles ( $p < 0.4$ ) (Figure 3B). Previous studies have noted an overall tendency for dsDNA to transform *B. subtilis* more effectively than ssDNA at neutral pH, but reported transformant counts were about 1–2 orders of magnitude greater for dsDNA than ssDNA.<sup>64</sup> This is comparable to differences observed here in particle-free systems. No significant difference in transformation frequency was detected between HASP and HASNP systems for dsDNA ( $p < 0.2$ ) or ssDNA ( $p < 0.07$ ).

**3.1.4. Particle-Associated Transformation via Various eARGs.** Significant differences in transformation frequency between the three genes were observed for HASNP ( $p < 0.0002$ ), HASP ( $3.6 \times 10^{-6}$ ), and particle-free systems ( $p < 0.0008$ ) (Figure 3C). This implies that transformation rates vary greatly between eARGs with different mutations and that particle-effects have comparatively less influence. In particle-free systems, *sul* genes have the highest  $f$  values, followed by *blt* and then by *dfrA24*. *dfrA24* is a chromosomal gene with multiple mutations, whereas *blt*, also a chromosomal gene, has a single mutation. It is possible that recipient cells require less metabolic energy to express plasmid-encoded *sul*, which does not require chromosomal integration for expression,<sup>19</sup> as opposed to chromosomal eARGs. Further, incorporating multiple mutations into the genome requires larger segments of DNA to be recombined into the recipient cell chromosome and therefore greater energy cost and sequence homology. This may explain why frequencies are higher for *blt* as compared to *dfrA24*.

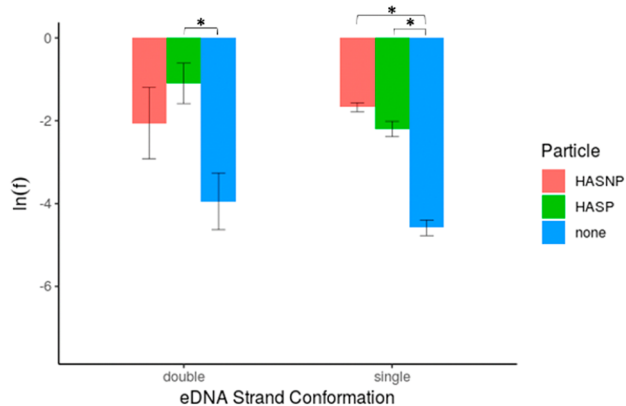
Transformation frequencies significantly increase with the addition of HASNPs ( $p < 8 \times 10^{-6}$  for *blt*,  $p < 0.03$  for *dfrA24*) or HASPs ( $p < 3.05 \times 10^{-10}$  for *blt*,  $p < 0.02$  for *dfrA24*), with no significant difference observed between them ( $p < 0.09$  for *blt*,  $p < 0.5$  for *dfrA24*). This demonstrates the ability of particles, including NPs, to improve transformability of multiple types of environmentally relevant chromosomal eARGs.

Transformations via *sul*, on the other hand, are not significantly impacted by the addition of either HASNPs ( $p < 0.2$ ) or HASPs ( $p < 0.06$ ). In previous studies, plasmids in soil have demonstrated lower transforming activity than chromosomal genes, even when they remain physically

(A)



(B)



(C)

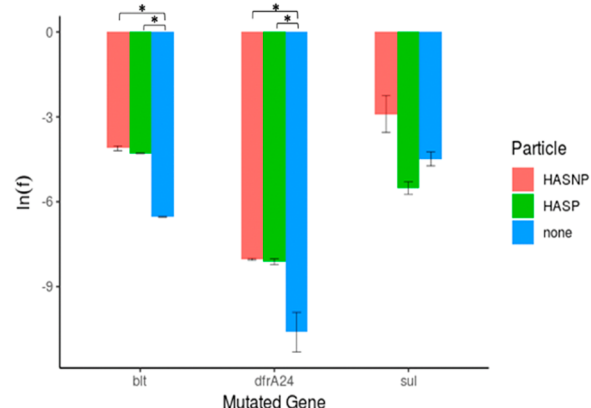


**Figure 3.** Transformation frequencies ( $f$ ) upon exposure to eARG fragments of (A) various sizes and (B) various strand conformations and (C) various mutated eARGs in systems with HASNPs, HASPs, or no particles. \*Denotes statistically significant difference between groups determined by a  $p$  value  $<0.05$ .

stable.<sup>65</sup> Some part of particle association may inhibit the transformability of plasmid DNA.

**3.2. Particle Aggregation Modeling.** **3.2.1. Model Predictions.** The calibration of the model using  $\alpha$  as a fitting parameter yielded  $\alpha$  values (given in the Supporting Information, Table S4) on the order of magnitude of those

documented in previous experiments.<sup>66</sup> Therefore, the calibration step was considered to provide reasonable corrections.

During validation with the HASP data set, the model predicted a  $T$  value within 35% of the experimental result. The  $T$  measured in HASP systems was  $0.0153 \text{ kg/m}^3$ , whereas the model predicted a  $T$  of  $\sim 0.010 \text{ kg/m}^3$ . Considering the simplifications applied to the model, the difference between the predicted and experimental  $T$  was acceptable for the purposes of validation, confirming the ability of particle aggregation theory to closely predict bacterial transformation rates.

The model has a unique value in its capacity to assess particle-level interactions that may govern the transfer of genes on particles. Possible contributions of various collision mechanisms ( $\beta$ ) leading to the association of genes and bacteria are shown in Figure 4 below.

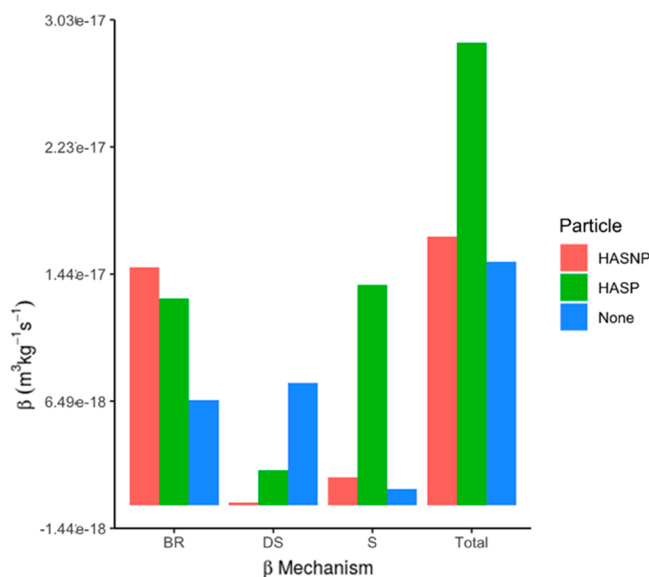


**Figure 4.** Contribution of Brownian motion (BR), differential settling (DS), and shear forces (S) on collision frequencies ( $\beta$ ) between bacteria and particle-bound and free eARGs.

Collisions between bacteria and free or NP-bound eARGs are predicted to be dominated by Brownian motion (Figure 4). For HASP-bound genes, shear forces increase greatly and override Brownian motion as the most dominant force, as expected. In the rectilinear model (at slow mixing and ambient temperature), Brownian motion is the predictably dominant mechanism of collision when particles are  $<1 \mu\text{m}$ , while shear dominates for larger particles.<sup>67</sup> The model also estimates that total collisions increase when particles are added and are greatest for the micron-sized particle compared to the NP. However, the rectilinear model is known to overpredict collision frequencies, particularly for larger particles.<sup>67</sup>

**3.2.2. Model Limitations.** To estimate adsorption parameters for HASPs where data was unavailable, the model assumes that adsorption is proportional to particle surface area. In reality, adsorption may be dependent on various factors. A uniform particle size for each particle type is also assumed, even though particles may have varying sizes due to heterogeneous humic acid sorption on the particle surface. Additionally, the attachment efficiency parameter  $\alpha_{LB}$  was calibrated for HASNP systems but is applied to HASP systems.

In reality,  $\alpha$  may vary based on particle size, surface chemistry, sorption capacity of eARGs, and more. Variations in  $\alpha$  may also be due to assumptions inherent to the rectilinear model, which tends to overpredict collisions for larger particles,<sup>32</sup> and this would be reflected in the  $\alpha$  calibration. There were also simplifications to the biology of the system, such as the assumptions of no growth or decay, consistent  $\gamma$ , lack of consideration of gene properties, gene expression, cellular competence, ROS production, DNA conformation, and more. As previously stated, the assumption of spherical particles following rectilinear collision trajectories may also distort the calculated interactions between particulate objects that are inherently nonspherical.

**3.2.3. Sensitivity Analysis.** Though complex biological factors cannot easily be incorporated into the model, the contribution of assumptions about particle size, attachment efficiency, and partition coefficient to model underpredictions were assessed. The values of  $d_L$ ,  $\alpha_{LB}$ , and  $P$  were iterated to determine the extent to which these parameters caused variations between model-predicted and experimental  $T$  values for HASP systems.

Considering Figure 5A,  $T$  at 90 min can be reached with a  $d_L$  of less than 180 nm. However, this is not a realistic diameter for HASPs, because the silica nanosphere core is manufactured to be 1  $\mu\text{m}$  in diameter. Therefore, the possible variation between the measured and actual diameter of particles does not entirely explain discrepancies between the model and experimental  $T$  predictions.

$T$  is also not particularly sensitive to  $\alpha_{LB}$  (Figure 5B), suggesting that assumptions inherent to  $\alpha$  do not particularly influence the effectiveness of the model. It can be concluded, then, that the rectilinear model may be a suitable framework to predict particle-mediated gene transfer processes since collision overpredictions influencing  $\alpha_{LB}$  would not significantly alter the model outcome. Of the parameters considered, the model is most sensitive to  $P$  (Figure 5C). It is evident that without changes to  $d_L$ , a  $P$  value between 0 and 0.1 could lead to a prediction of  $T$  equal to the experimental value (0.0153  $\text{kg}/\text{m}^3$ ).

The sensitivity of the model to  $d_L$  and  $P$  implies that the assumptions used to calculate these parameters are likely major contributors to deviations between model-predicted and experimental values. In experiments, the size of the particle does not significantly impact  $T$  at 1  $\mu\text{g}/\text{mL}$  DNase I (Figure 2), but the model predicts a large difference in  $T$  based on particle size. The model, therefore, overpredicts the role of particle surface area. This may also be due to the model's inability to account for other simultaneous processes, such as eARG conformation changes.

**3.2.4. Environmental Implications.** This work establishes the ability of naturally occurring NP-associated genetic material to confer resistance to bacterial populations via natural transformation. This is an initial step in revealing how the interactions of eARGs with environmental components may facilitate the transfer of resistance among microbial populations and implies that association with nanoparticles may be particularly important. The implications of this work are limited by the simplified system used, which did not account for various complex biological and environmental factors such as microbial diversity or variations in concentration of available nucleases. Therefore, further study is required to extrapolate the observed eARG–NP–bacteria interactions to realistic and complex environments. This may

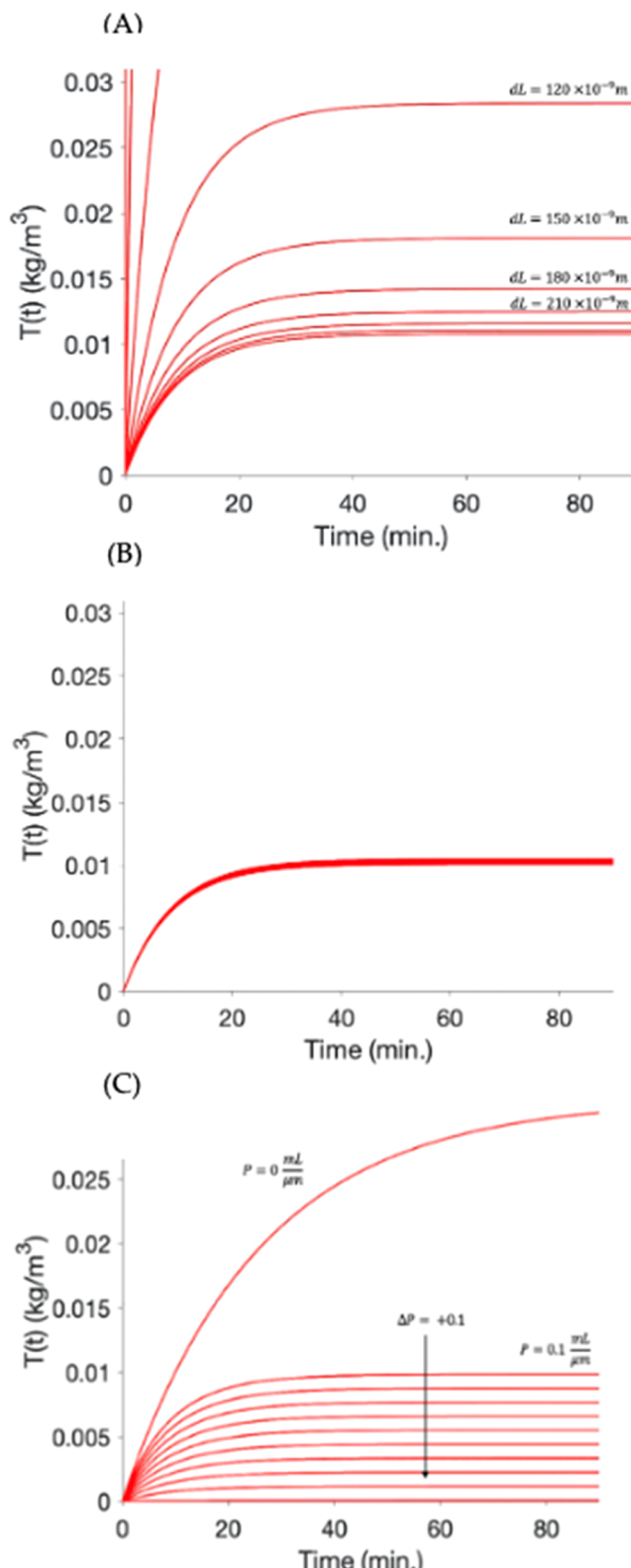


**Figure 5.** Sensitivity of the model to (A) the eARG–particle complex diameter,  $d_L$ , (B) attachment efficiency between particle bound eARG and bacteria,  $\alpha_{LB}$ , and (C) partition coefficient,  $P$ , during adsorption.

allow an eventual understanding of how eARG behavior may regulate the spread of antibiotic resistance. This understanding may have implications for the tracking and characterization of antibiotic resistance in the environment.

The ability to model this phenomenon is also a step in better understanding the role eARGs play in propagating resistance. The developed model was capable of broadly predicting transformation frequencies in various conditions. This capacity implies that classical particle aggregation theory could be a useful tool for quantifying extracellular gene uptake by microbes. The model is limited by some unaccounted biological factors, such as the possible differences in transformation factor ( $\gamma$ ) based on where the eDNA is free or particle bound or ROS production. This approach is valuable because, though subject to limitations, it allows for a simplified calculation based on available data that can closely predict transformation rates. It provides the ability to test effects of simple modifications in gene or particle properties on bioavailability. Such a model may realistically be incorporated into larger and more comprehensive simulations that assess the spread of antibiotic resistance in the environment.

## ASSOCIATED CONTENT

### Supporting Information

The Supporting Information is available free of charge at <https://pubs.acs.org/doi/10.1021/acs.est.2c02878>.

Genetic sequences of eARG fragments and primers, DNA and particle preparation procedures, particle characterization methods and data, transformation assay procedures, detailed calculations for model formulation, bacterial growth curve, model parameters, and MAT-LAB code for the model ([PDF](#))

## AUTHOR INFORMATION

### Corresponding Author

Nadratun N. Chowdhury – Department of Civil and Environmental Engineering, Duke University, Durham, North Carolina 27708, United States;  [orcid.org/0000-0003-2336-5902](https://orcid.org/0000-0003-2336-5902); Email: [nnc4@duke.edu](mailto:nnc4@duke.edu)

### Authors

Ethan Hicks – Department of Civil and Environmental Engineering, Duke University, Durham, North Carolina 27708, United States

Mark R. Wiesner – Department of Civil and Environmental Engineering, Duke University, Durham, North Carolina 27708, United States;  [orcid.org/0000-0002-0823-5045](https://orcid.org/0000-0002-0823-5045)

Complete contact information is available at:

<https://pubs.acs.org/10.1021/acs.est.2c02878>

### Notes

The authors declare no competing financial interest.

## ACKNOWLEDGMENTS

This material is based upon work supported by the National Science Foundation GRFP Grant 1644868. This work was also partially funded through the Center for the Environmental Implications of NanoTechnology (CEINT) under NSF Cooperative Agreement Number EF-0830093 and the Duke University Superfund Research Center under the NIEHS Grant T32ES021432.

## REFERENCES

- (1) He, H.; Zhou, P.; Shimabuku, K.; Fang, X.; Li, S.; Lee, Y.; Dodd, M. Degradation and Deactivation of Bacterial Antibiotic Resistance Genes During Exposure to Free Chlorine, Monochloramine, Chlorine Dioxide, Ozone, Ultraviolet Light, and Hydroxyl Radical. *Environ. Sci. Technol.* **2019**, *53*, 2013–2026.
- (2) Allen, H. K.; Donato, J.; Wang, H. H.; Cloud-Hansen, K. A.; Davies, J.; Handelsman, J. Call of the wild: antibiotic resistance genes in natural environments. *Nature Reviews Microbiology* **2010**, *8*, 251–259.
- (3) Magee, J. T.; Pritchard, E. L.; Fitzgerald, K. A.; Dunstan, F. D. J.; Howard, A. J. Antibiotic prescribing and antibiotic resistance in community practice: retrospective study. *British Medical Journal* **1999**, *319*, 1239–1240.
- (4) Martínez, J. L. Antibiotics and antibiotic resistance genes in natural environments. *Science* **2008**, *321* (5887), 365–367.
- (5) Vikesland, P. J.; Pruden, A.; Alvarez, P. J. J.; Aga, D.; Burgmann, H.; Li, X.-d.; Manaia, C. M.; Nambi, I.; Wigginton, K.; Zhang, T.; Zhu, Y.-G. Toward a Comprehensive Strategy to Mitigate Dissemination of Environmental Sources of Antibiotic Resistance. *Environ. Sci. Technol.* **2017**, *51*, 13061–13069.
- (6) Pruden, A.; Pei, R.; Storteboom, H.; Carlson, K. H. Antibiotic resistance genes as emerging contaminants: studies in northern Colorado. *Environ. Sci. Technol.* **2006**, *40*, 7445–7450.
- (7) Guo, X. P.; Yang, Y.; Lu, D. P.; Niu, Z. S.; Feng, J. N.; Chen, Y. R.; Tou, F. Y.; Garner, J.; Xu, J.; Liu, M.; Hochella, M. F. J. Biofilms as a sink for antibiotic resistance genes (ARGs) in the Yangtze Estuary. *Water Res.* **2018**, *129*, 277–286.
- (8) Wang, D. N.; Liu, L.; Qiu, Z. G.; Shen, Z. Q.; Guo, X.; Yang, D.; Li, J.; Liu, W. I.; Jin, M.; Li, J. W. A new adsorption-elution technique for the concentration of aquatic extracellular antibiotic resistance genes from large volumes of water. *Water Res.* **2016**, *92*, 188–198.
- (9) Bien, T. L. T.; Thao, N. V.; Kitamura, S. I.; Obayashi, Y.; Suzuki, S. Release and constancy of an antibiotic resistance gene in seawater under grazing stress by ciliates and heterotrophic nanoflagellates. *Microbes and Environments* **2017**, *32*, 174–179.
- (10) Mao, D.; Luo, Y.; Mathieu, J.; Wang, Q.; Feng, L.; Mu, Q.; Feng, C.; Alvarez, P. J. J. Persistence of Extracellular DNA in River Sediment Facilitates Antibiotic Resistance Gene Propagation. *Environ. Sci. Technol.* **2014**, *48*, 71–78.
- (11) Yuan, K.; Wang, X.; Chen, X.; Zhao, Z.; Fang, L.; Chen, B.; Jiang, J.; Luan, T.; Chen, B. Occurrence of antibiotic resistance genes in extracellular and intracellular DNA from sediments collected from two types of aquaculture farms. *Chemosphere* **2019**, *234*, 520.
- (12) McKinney, C. W.; Loftin, K. A.; Meyer, M. T.; Davis, J. G.; Pruden, A. tet and sul Antibiotic Resistance Genes in Livestock Lagoons of Various Operation Type, Configuration, and Antibiotic Occurrence. *Environ. Sci. Technol.* **2010**, *44* (16), 6102–6109.
- (13) Xi, C.; Zhang, Y.; Marrs, C. F.; Ye, W.; Simon, C.; Foxman, B.; Nriagu, J. Prevalence of antibiotic resistance in drinking water treatment and distribution systems. *Applied and environmental microbiology* **2009**, *75* (17), 5714–5718.
- (14) Gardner, C.; Volkoff, S.; Gunsch, C. Examining the behavior of crop-derived antibiotic resistance genes in anaerobic sludge batch reactors under thermophilic conditions. *Biotechnol. Bioeng.* **2019**, *116* (11), 3063–3071.
- (15) Lu, Y.; Xiao, Y.; Zheng, G.; Lu, J.; Zhou, L. Conditioning with zero-valent iron or Fe<sup>2+</sup> activated peroxydisulfate at an acidic initial sludge pH removed intracellular antibiotic resistance genes but increased extracellular antibiotic resistance genes in sewage sludge. *Journal of Hazardous Materials* **2020**, *386*, 121982.
- (16) Zhang, Y.; Li, A.; Dai, T.; Li, F.; Xie, H.; Chen, L.; Wen, D. Cell-free DNA: a neglected source for antibiotic resistance genes spreading from WWTPs. *Environ. Sci. Technol.* **2018**, *52*, 248–257.
- (17) Rizzo, L.; Manaia, C.; Merlin, C.; Schwartz, T.; Dagot, C.; Ploy, M. C.; Michael, I.; Fatta-Kassinos, D. Urban wastewater treatment plants as hotspots for antibiotic resistant bacteria and genes spread into the environment: a review. *Sci. Total Environ.* **2013**, *447*, 345–360.
- (18) Pietramellara, G.; Ascher, J.; Borgogni, F.; Ceccherini, M. T.; Guerri, G.; Nannipieri, P. Extracellular DNA In Soil And Sediment: Fate And Ecological Relevance. *Biology and Fertility of Soils* **2009**, *45*, 219–235.

(19) Lorenz, M. G.; Wackernagel, W. Bacterial Gene Transfer by Natural Genetic Information in the Environment. *Microbiological Reviews* 1994, 58 (3), 563–602.

(20) Stewart, G. J.; Sinigalliano, C. D. Detection of horizontal gene transfer by natural transformation in native and introduced species of bacteria in marine and synthetic sediments. *Appl. Environ. Microbiol.* 1990, 56 (6), 1818–1824.

(21) Nagler, M.; Insam, H.; Pietramellara, G.; Ascher-Jenull, J. Extracellular DNA in natural environments: features, relevance and applications. *Appl. Microbiol. Biotechnol.* 2018, 102, 6343.

(22) Blum, S. A. E.; Lorenz, M. G.; Wackernagel, W. Mechanism of retarded DNA degradation and prokaryotic origin of DNases in non-sterile soils. *Systems Applied Microbiology* 1997, 20, 513–521.

(23) Sikorski, J.; Graupner, S.; Lorenz, M. G.; Wackernagel, W. Natural genetic transformation of *Pseudomonas stutzeri* in a non-sterile soil. *Microbiology* 1998, 144 (2), 569–576.

(24) Khanna, M.; Stotzky, G. Transformation of *Bacillus subtilis* by DNA Bound on Montmorillonite and Effect of DNase on the Transforming Ability of Bound DNA. *Appl. Environ. Microbiol.* 1992, 58, 1930–1939.

(25) Demaneche, S.; Jocteur-Monrozier, L.; Quiquampoix, H.; Simonet, P. Evaluation of biological and physical protection against nucleic acid degradation of clay-bound plasmid DNA. *Appl. Environ. Microbiol.* 2001, 67, 293–299.

(26) Crecchio, C.; Stotzky, G. Binding of DNA on humic acids: effect on transformation of *Bacillus subtilis* and resistance to DNase. *Soil Biology and Biochemistry* 1998, 30, 1061–1067.

(27) Lorenz, M.; Wackernagel, W. Adsorption of DNA to sand and variable degradation rates of adsorbed DNA. *Appl. Environ. Microbiol.* 1987, 53, 2948–2952.

(28) Chowdhury, N. N.; Cox, A. R.; Wiesner, M. R. Nanoparticles as vectors for antibiotic resistance: The association of silica nanoparticles with environmentally relevant extracellular antibiotic resistance genes. *Science of The Total Environment* 2021, 761, 143261.

(29) Chowdhury, N. N.; Wiesner, M. R. Persistence and Environmental Relevance of Extracellular Antibiotic Resistance Genes: Regulation by Nanoparticle Association. *Environmental Engineering Science* 2021, 38, 1129.

(30) Wiesner, M.; Lowry, G.; Alvarez, P.; Dionysiou, D.; Biswas, P. Assessing the Risks of Manufactured Nanomaterials. *Environ. Sci. Technol.* 2006, 40 (14), 4336–4345.

(31) Schwab, F.; Zhai, G.; Kern, M.; Turner, A.; Schnoor, J. L.; Wiesner, M. Barriers, pathways and processes for uptake, translocation and accumulation of nanomaterials in plants—Critical review. *Nanotoxicology* 2016, 10 (3), 257–278.

(32) Smoluchowski, M. Versuch einer mathematischen Theorie der Koagulationskinetik kolloider Lösungen. *Z. Phys. Chem.* 1917, 92, 129–168.

(33) Worley-Morse, T. O.; Gunsch, C. K. Modeling phage induced bacterial disinfection rates and the resulting design implications. *Water Res.* 2015, 68, 627–636.

(34) Hicks, E.; Wiesner, M. R.; Gunsch, C. K. Modeling bacteriophage-induced inactivation of *Escherichia coli* utilizing particle aggregation kinetics. *Water Res.* 2020, 171, 115438.

(35) Arabi, H.; Pakzad, I.; Nasrollahi, A.; Hosainzadegan, H.; Azizi Jalilian, F.; Taherikalani, M.; Samadi, N.; Monadi Sefidan, A. Sulfonamide Resistance Genes (sul) M in Extended Spectrum Beta Lactamase (ESBL) and Non-ESBL Producing *Escherichia coli* Isolated From Iranian Hospitals. *Jundishapur J. Microbiol.* 2015, 8 (7), e19961.

(36) Sánchez-Osuna, M.; Cortés, P.; Barbé, J.; Erill, I. Origin of the Mobile Di-Hydro-Pteroate Synthase Gene Determining Sulfonamide Resistance in Clinical Isolates. *Frontiers in Microbiology* 2019, 9, 3332.

(37) Mathys, V.; Wintjens, R.; Lefevre, P.; Bertout, J.; Singhal, A.; Kiass, M.; Kurepina, N.; Wang, X.-M.; Mathema, B.; Baulard, A.; Kreiswirth, B. N.; Bifani, P. Molecular genetics of para-aminosalicylic acid resistance in clinical isolates and spontaneous mutants of *Mycobacterium tuberculosis*. *Antimicrob. Agents Chemother.* 2009, 53 (5), 2100–2109.

(38) Brolund, A.; Sundqvist, M.; Kahlmeter, G.; Grape, M. Molecular Characterisation of Trimethoprim Resistance in *Escherichia coli* and *Klebsiella pneumoniae* during a Two Year Intervention on Trimethoprim Use. *PLoS One* 2010, 5, e9233.

(39) Chowdhury, N. N.; Wiesner, M. R. Persistence and Environmental Relevance of Extracellular Antibiotic Resistance Genes: Regulation by Nanoparticle Association. *Environmental Engineering Science* 2021, 38 (12), 1129–1139.

(40) Cai, P.; Huang, Q.; Zhang, X. Interactions of DNA with Clay Minerals and Soil Colloidal Particles and Protection Against Degradation by DNase. *Environ. Sci. Technol.* 2006, 40, 2971–2976.

(41) Dubnau, D. DNA uptake in bacteria. *Annual Reviews Microbiology* 1999, 53, 217–244.

(42) Seto, H.; Lopez, R.; Tomasz, A. Cell surface-located deoxyribonucleic acid receptors in transformable pneumococci. *Journal of bacteriology* 1975, 122 (3), 1339–1350.

(43) Smith, H. O.; Danner, D. B.; Deich, R. A. Genetic Transformation. *Annu. Rev. Biochem.* 1981, 50 (1), 41–68.

(44) Fitzmaurice, W. P.; Benjamin, R. C.; Huang, P. C.; Scocca, J. J. Characterization of recognition sites on bacteriophage HP1c1 DNA which interact with the DNA uptake system of *Haemophilus influenzae* Rd. *Gene* 1984, 31 (1), 187–196.

(45) Garcia, E.; Lopez, P.; Ureña, M. T.; Espinosa, M. Early stages in *Bacillus subtilis* transformation: association between homologous DNA and surface structures. *Journal of bacteriology* 1978, 135 (3), 731–740.

(46) Eisenstadt, E.; Lange, R.; Willecke, K. Competent *Bacillus subtilis* cultures synthesize a denatured DNA binding activity. *Proc. Natl. Acad. Sci. U. S. A.* 1975, 72 (1), 323–327.

(47) Kieft, T. L.; Caldwell, D. E. Chemostat and in-situ colonization kinetics of *thermotrichia thiopara* on calcite and pyrite surfaces. *Geomicrobiology Journal* 1984, 3 (3), 217–229.

(48) Jeffrey, W. H.; Paul, J. H. Activity of an Attached and Free-Living *Vibrio* sp. as Measured by Thymidine Incorporation, p-Iodonitrotetrazolium Reduction, and ATP/DNA Ratios. *Applied and environmental microbiology* 1986, 51 (1), 150–156.

(49) Caldwell, D. E.; Lawrence, J. R. Growth Kinetics of *Pseudomonas fluorescens* Microcolonies within the Hydrodynamic Boundary Layers of Surface Microenvironments. *Microbial Ecology* 1986, 12 (3), 299–312.

(50) Chamier, B.; Lorenz, M. G.; Wackernagel, W. Natural Transformation of *Acinetobacter calcoaceticus* by Plasmid DNA Adsorbed on Sand and Groundwater Aquifer Material. *Applied and environmental microbiology* 1993, 59 (5), 1662–1667.

(51) Crecchio, C.; Ruggiero, P.; Curci, M.; Colombo, C.; Palumbo, G.; Stotzky, G. Binding of DNA from *Bacillus subtilis* on montmorillonite-humic acids-aluminum or iron hydroxypolymers: effects on transformation and protection against DNase. *Soil Science Society* 2005, 69, 834–841.

(52) Lorenz, M. G.; Aardema, B. W.; Wackernagel, W. Highly Efficient Genetic Transformation of *Bacillus subtilis* Attached to Sand Grains. *Microbiology* 1988, 134 (1), 107–112.

(53) Cui, H.; Smith, A. L. Impact of engineered nanoparticles on the fate of antibiotic resistance genes in wastewater and receiving environments: A comprehensive review. *Environmental Research* 2022, 204, 112373.

(54) Qiu, Z.; Shen, Z.; Qian, D.; Jin, M.; Yang, D.; Wang, J.; Zhang, B.; Yang, Z.; Chen, Z.; Wang, X.; Ding, C.; Wang, D.; Li, J.-W. Effects of nano-TiO<sub>2</sub> on antibiotic resistance transfer mediated by RP4 plasmid. *Nanotoxicology* 2015, 9 (7), 895–904.

(55) Liu, X.; Tang, J.; Song, B.; Zhen, M.; Wang, L.; Giesy, J. P. Exposure to Al<sub>2</sub>O<sub>3</sub> nanoparticles facilitates conjugative transfer of antibiotic resistance genes from *Escherichia coli* to *Streptomyces*. *Nanotoxicology* 2019, 13 (10), 1422–1436.

(56) Wang, X.; Yang, F.; Zhao, J.; Xu, Y.; Mao, D.; Zhu, X.; Luo, Y.; Alvarez, P. J. J. Bacterial exposure to ZnO nanoparticles facilitates horizontal transfer of antibiotic resistance genes. *NanoImpact* 2018, 10, 61–67.

(57) Lu, J.; Wang, Y.; Jin, M.; Yuan, Z.; Bond, P.; Guo, J. Both silver ions and silver nanoparticles facilitate the horizontal transfer of plasmid-mediated antibiotic resistance genes. *Water Res.* **2020**, *169*, 115229.

(58) Carlos, L.; Pedersen, B. W.; Ogilby, P. R.; Martire, D. O. The role of humic acid aggregation on the kinetics of photosensitized singlet oxygen production and decay. *Photochemical & Photobiological Sciences* **2011**, *10* (6), 1080–1086.

(59) Miao, R.; Guild, W. R. Competent *Diplococcus pneumoniae* accept both single- and double-stranded deoxyribonucleic acid. *Journal of bacteriology* **1970**, *101* (2), 361–364.

(60) Morrison, D. A.; Guild, W. R. Transformation and deoxyribonucleic acid size: extent of degradation on entry varies with size of donor. *Journal of bacteriology* **1972**, *112* (3), 1157–1168.

(61) van Dijk, B.; Hogeweg, P.; Doekes, H. M.; Takeuchi, N. Slightly beneficial genes are retained by bacteria evolving DNA uptake despite selfish elements. *eLife* **2020**, *9*, e56801.

(62) Overballe-Petersen, S.; Harms, K.; Orlando, L. A. A.; Mayar, J. V. M.; Rasmussen, S.; Dahl, T. W.; Rosing, M. T.; Poole, A. M.; Sicheritz-Ponten, T.; Brunak, S.; Inselmann, S.; de Vries, J.; Wackernagel, W.; Pybus, O. G.; Nielsen, R.; Johnsen, P. J.; Nielsen, K. M.; Willems, E. Bacterial natural transformation by highly fragmented and damaged DNA. *Proc. Natl. Acad. Sci. U. S. A.* **2013**, *110* (49), 19860–19865.

(63) Domingues, S.; Harms, K.; Fricke, W. F.; Johnsen, P. J.; da Silva, G. J.; Nielsen, K. M. Natural transformation facilitates transfer of transposons, integrons and gene cassettes between bacterial species. *PLoS Pathog* **2012**, *8* (8), e1002837.

(64) Tevethia, M. J.; Mandel, M. Effects of pH on transformation of *Bacillus subtilis* with single-stranded deoxyribonucleic acid. *Journal of bacteriology* **1971**, *106* (3), 802–807.

(65) Romanowski, G.; Lorenz, M. G.; Sayler, G.; Wackernagel, W. Persistence of free plasmid DNA in soil monitored by various methods, including a transformation assay. *Applied and environmental microbiology* **1992**, *58* (9), 3012–3019.

(66) Barton, L.; Therezien, M.; Auffan, M.; Bottero, J.-Y.; Wiesner, M. Theory and Methodology for Determining Nanoparticle Affinity for Heteroaggregation in Environmental Matrices Using Batch Measurements. *Environmental Engineering Science* **2014**, *31* (7), 421.

(67) Han, M.; Lawler, D. F. The (Relative) Insignificance of G in Flocculation. *Journal (American Water Works Association)* **1992**, *84* (10), 79–91.

## □ Recommended by ACS

### Enhanced Bacterial Growth by Polyelemental Glycerolate Particles

Abhijit H. Phakatkar, Reza Shahbazian-Yassar, *et al.*

MARCH 18, 2023

ACS APPLIED BIO MATERIALS

READ 

### Biofilm-Colonized versus Virgin Black Microplastics to Accelerate the Photodegradation of Tetracycline in Aquatic Environments: Analysis of Underneath Mechanisms

Rui Ding, Lingyan Zhu, *et al.*

MARCH 30, 2023

ENVIRONMENTAL SCIENCE & TECHNOLOGY

READ 

### Inhibition of Biofilm and Virulence Properties of Pathogenic Bacteria by Silver and Gold Nanoparticles Synthesized from *Lactiplantibacillus* sp. Strain C1

Min-Gyun Kang, Young-Mog Kim, *et al.*

MARCH 07, 2023

ACS OMEGA

READ 

### Structural Characteristics and Functional Genes of Biofilms in Microbial Electrolysis Cells for Chlorobenzene Abatement

Zanyun Ying, Shihan Zhang, *et al.*

JANUARY 19, 2023

ACS ES&T WATER

READ 

Get More Suggestions >